

## CHAPTER 6. BULK ROCK GEOCHEMISTRY

---

### 6.1 General

The major oxides, trace as well as rare earth elements (REEs) concentrations present within the seventeen representative calc-silicate rock samples of the study area were obtained by geochemical analyses. Major oxide data acquired using Wavelength Dispersive X-Ray Fluorescence (WD-XRF) using Philips MagiX PRO model PW 2440 wavelength dispersive X-ray fluorescence spectrometer coupled with automatic sample changer PW 2540, while trace elements and rare-earth elements (REEs) have been analysed using High Resolution Inductively Coupled Plasma Mass Spectrometer (HR-ICP-MS; Nu Instruments Attom, UK) at the CSIR National Geophysical Research Institute, Hyderabad, following acid digestion that involves repeated treatment with HF-HNO<sub>3</sub>-HClO<sub>4</sub>. SARM-40 (South Africa) was used as standard. Analytical results for major, trace and rare-earth elements are presented in Table 6.1.

### 6.2 Major elements compositions

Major oxides data of these calc-silicates exhibit a range of SiO<sub>2</sub> (51.4-64.9 wt.%) and Al<sub>2</sub>O<sub>3</sub> (7.8-13.1 wt.%) which is lower than the average composition of post-archean upper continental crust (PAUCC), i.e 65.9% and 15.17% respectively of Taylor and McLennan (1985) whereas MgO (5.7-15.6 wt.%), CaO (5.4-13.5 wt.%), FeO (3.7-6.9 wt.%), and MnO (0.1-0.4 wt.%) whole-rock compositions show enrichment relative to the compositions of PAUCC. Plots of weight % SiO<sub>2</sub> versus major oxides show that Al<sub>2</sub>O<sub>3</sub>, Na<sub>2</sub>O, K<sub>2</sub>O and TiO<sub>2</sub> values are positively correlated with SiO<sub>2</sub> content in all of the samples whereas CaO, MgO, FeO, MnO, P<sub>2</sub>O<sub>5</sub> and LOI are inversely correlated with SiO<sub>2</sub> (Fig.6.1). Major-elements Si, Al, Fe, Ca, and Mg are the most abundant whole-rock constituents in calc-silicates of Lunavada area.

---

\* The part of this chapter is based on our paper published:

Akolkar G and Limaye M A 2020 Geochemistry of calc-silicate rocks around Lunavada region, NE Gujarat: Implications for their protolith, provenance and tectonic setting; *Journal of Earth System Sciences* **129** 198. <https://doi.org/10.1007/s12040-020-01463-4>.

Table 6.1: Major (wt%), trace and rare earth element (ppm) analyses of the representative calc-silicate rock samples

Sample No.	GCSL-1	GCSL-2	GCSL-3	GCSL-4	GCSL-5	GCSL-6	GCSL-7	GCSL-8	GCSL-9
Lat.	23°5'48.9''	23°5'11.3''	23°04'56.9''	23°04'51.2''	23°03'30.1''	23°03'31.1''	23°4'1.5''	23°4'1.7''	23°3'13.1''
Long.	73°43'17.8''	73°43'0.1''	73°42'27.6''	73°42'14.2''	73°40'11.5''	73°40'20.5''	73°39'51.5''	73°39'51.6''	73°40'20.9''
SiO <sub>2</sub>	58.98	58.51	51.36	52.66	64.87	56.97	57.94	51.85	62.96
Al <sub>2</sub> O <sub>3</sub>	13.15	12.13	8.46	9.18	7.82	8.46	8.85	8.36	12.98
FeO	5.15	5.38	5.95	5.24	3.66	5.23	5.52	6.95	4.41
MnO	0.13	0.19	0.37	0.35	0.25	0.27	0.21	0.39	0.13
MgO	7.27	8.43	15.59	13.39	5.99	11.47	10.88	14.99	5.73
CaO	6.76	7.18	13.50	12.99	12.72	10.11	10.70	12.56	5.42
Na <sub>2</sub> O	1.31	0.80	0.80	0.93	0.28	0.81	2.25	0.80	1.48
K <sub>2</sub> O	3.02	3.51	1.80	1.95	0.29	2.81	0.53	1.58	3.39
TiO <sub>2</sub>	0.79	0.82	0.51	0.58	0.84	0.57	0.67	0.48	0.72
P <sub>2</sub> O <sub>5</sub>	0.24	0.16	0.24	0.16	0.24	0.17	0.17	0.20	0.14
LOI	0.71	0.54	0.44	0.48	0.62	0.63	0.44	0.55	0.69
Sum	98.15	98.32	99.76	98.56	98.04	98.15	98.85	99.58	98.3
Sc	8.01	9.18	9.29	7.54	11.09	8.49	8.53	10.78	8.03
V	49.47	60.0	67.14	35.28	74.48	66.60	54.60	74.45	54.81
Cr	41.46	73.29	43.45	65.47	56.90	52.60	51.35	45.29	59.04
Co	15.45	20.52	24.46	18.49	18.91	22.06	20.35	24.17	17.15
Ni	24.56	33.59	27.31	28.66	28.32	30.42	25.28	28.46	27.48
Cu	11.40	18.41	10.81	14.52	13.12	13.19	11.88	10.26	12.90
Zn	61.42	89.62	91.05	61.22	59.91	74.23	86.09	85.58	57.14
Ga	50.29	44.48	34.32	27.60	43.83	36.55	42.59	45.22	46.27
Rb	946.11	1332.22	603.68	101.44	762.40	636.36	241.58	499.16	1270.60
Sr	144.83	124.83	131.09	206.35	167.51	101.60	154.51	142.073	155.33
Y	43.07	34.90	27.82	57.91	36.53	30.65	38.23	31.033	29.42
Zr	465.99	299.42	201.76	467.82	292.68	343.69	320.98	187.75	295.94
Nb	22.09	23.16	17.19	29.86	19.08	23.36	24.64	17.16	18.14
Cs	6.68	9.45	5.61	0.50	7.08	1.99	1.34	2.883	11.038
Ba	1378.68	1820.08	1115.28	156.23	1791.01	1714.9	206.46	1218.23	2076.58

La	46.19	29.75	23.70	60.41	30.36	22.13	38.6	26.31	32.06
Ce	95.91	61.09	48.75	126.23	69.69	46.06	79.04	53.78	65.58
Pr	10.20	6.57	5.43	13.69	6.92	4.97	8.68	6.017	6.97
Nd	40.36	25.71	22.14	53.95	27.48	20.09	34.93	24.15	27.35
Sm	8.35	5.45	4.85	11.17	5.99	4.36	7.38	5.19	5.70
Eu	1.50	1.04	0.93	1.72	1.17	0.84	1.31	0.96	1.00
Gd	6.70	4.75	4.18	8.99	5.02	3.95	5.96	4.35	4.63
Tb	1.18	0.87	0.75	1.57	0.95	0.77	1.043	0.79	0.80
Dy	7.63	5.9	4.95	9.95	6.41	5.36	6.69	5.26	5.22
Ho	1.66	1.34	1.10	2.12	1.45	1.18	1.46	1.17	1.11
Er	4.43	3.66	2.92	5.6	3.96	3.22	3.87	3.22	2.93
Tm	0.69	0.58	0.45	0.86	0.62	0.50	0.61	0.50	0.45
Yb	4.28	3.77	2.88	5.28	3.99	3.27	3.86	3.18	2.84
Lu	0.62	0.56	0.42	0.78	0.59	0.50	0.59	0.48	0.44
Hf	14.78	9.85	7.05	15.07	9.89	11.39	10.34	6.33	9.50
Ta	1.09	1.24	0.87	1.42	1.10	1.06	1.084	0.96	0.78
Pb	23.72	19.64	19.07	29.13	16.52	20.85	14.07	18.69	16.97
Th	47.89	41.83	27.13	66.58	33.65	35.92	38.21	26.29	37.28
U	2.25	1.99	1.37	3.05	1.47	1.63	2.09	0.99	1.94
(La/Sm) <sup>N</sup>	3.56	3.52	3.15	3.49	3.26	3.27	3.37	3.27	3.62
(Gd/Yb) <sup>N</sup>	1.29	1.04	1.2	1.4	1.04	0.99	1.27	1.13	1.34
(La/Yb) <sup>N</sup>	7.73	5.65	5.89	8.2	5.45	4.85	7.16	5.93	9.15
Eu/Eu*	0.593	0.614	0.617	0.51	0.636	0.61	0.58	0.6	0.58
Zr/Sc	58.1114	32.5918	21.7119	61.9711	26.3797	40.4539	37.59	17.40	36.82
Th/Sc	5.973	4.5531	2.91	8.8203	3.0336	4.2283	4.47	2.43	4.63
Th/Co	3.1	2.037	1.1	3.6	1.779	1.628	1.877	1.08	2.17
La/Th	0.964	0.711	0.873	0.907	0.902	0.616	1.01	1	0.86
La/Sc	5.76	3.238	2.55	8	2.736	2.6	4.52	2.43	3.99
Cr/Th	0.865	1.75	1.6	0.98	1.69	1.46	1.34	1.72	1.58

Sample No.	GCSL-10	GCSL-11	GCSL-12	GCSL-13	GCSL-14	GCSL-15	GCSL-16	GCSL-17
Lat.	23 <sup>0</sup> 3'14.1''	23 <sup>0</sup> 04'11.4''	23 <sup>0</sup> 03'27.1''	23 <sup>0</sup> 02'10.1''	23 <sup>0</sup> 03'30.1''	23 <sup>0</sup> 03'31.1''	23 <sup>0</sup> 4'1.5''	23 <sup>0</sup> 4'1.7''
Long.	73 <sup>0</sup> 40'25.1''	73 <sup>0</sup> 40'34.7''	73 <sup>0</sup> 40'14.6''	73 <sup>0</sup> 38'53.2''	73 <sup>0</sup> 40'11.5''	73 <sup>0</sup> 40'20.5''	73 <sup>0</sup> 39'51.5''	73 <sup>0</sup> 39'51.6''
SiO <sub>2</sub>	60.09	51.37	52.89	51.43	56.71	59.81	58.90	58.54
Al <sub>2</sub> O <sub>3</sub>	12.11	9.05	10.54	9.86	9.96	7.93	8.78	9.76
FeO	3.28	5.29	5.74	6.20	5.84	4.31	5.09	4.52
MnO	0.21	0.22	0.30	0.27	0.282	0.29	0.26	0.23
MgO	5.70	13.93	12.71	12.62	12.254	11.57	11.48	10.98
CaO	12.38	12.83	9.02	12.10	7.915	10.30	8.94	8.33
Na <sub>2</sub> O	2.91	0.86	0.53	0.66	0.669	0.51	1.23	1.21
K <sub>2</sub> O	0.39	2.48	3.11	1.94	2.71	2.104	1.9	2.35
TiO <sub>2</sub>	0.58	0.58	0.65	0.72	0.558	0.51	0.53	0.51
P <sub>2</sub> O <sub>5</sub>	0.17	0.15	0.16	0.20	0.157	0.15	0.16	0.13
LOI	0.68	0.91	2.05	1.65	1.28	0.9	0.71	1.13
Sum	98.91	98.33	98.42	98.42	99.03	98.94	98.61	98.24
Sc	7.60	9.37	9.80	9.38	20.92	11.22	17.29	13.74
V	43.98	62.16	63.75	63.57	88.29	66.26	101.31	82.007
Cr	47.73	47.15	47.39	48.61	207.50	147.29	164.79	132.43
Co	10.69	22.77	21.57	22.31	17.42	13.72	23.21	18.05
Ni	24.99	27.86	28.82	27.97	75.92	113.36	98.33	72.60
Cu	11.22	10.95	29.37	11.60	76.75	67.82	55.75	49.39
Zn	69.31	73.63	88.72	79.62	172.35	156.15	241.11	169.30
Ga	33.13	39.69	45.88	44.40	15.41	17.91	17.86	15.78
Rb	112.26	737.68	1547.79	637.37	106.61	256.14	134.14	73.76
Sr	200.29	122.2	90.16	124.96	177.17	183.74	174.64	160.23
Y	27.65	30.66	30.26	31.31	30.29	29.73	33.69	30.81
Zr	150.98	227.27	300.77	259.32	211.50	246.15	266.39	227.91
Nb	19.67	15.98	18.89	23.35	18.66	13.46	22.70	18.55
Cs	0.568	5.33	4.68	5.20	6.00	9.45	9.41	4.85
Ba	259.89	1533.56	1660.04	1445.19	106.65	385.83	139.50	87.25

La	28.11	29.09	27.17	19.72	31.10	64.17	28.16	32.90
Ce	60.05	59.86	61.01	40.60	62.20	122.00	56.39	65.68
Pr	6.61	6.57	5.87	4.44	7.46	13.96	6.80	7.89
Nd	25.78	26.17	23.24	17.86	27.68	48.59	25.58	29.21
Sm	5.57	5.54	4.97	3.95	5.68	8.54	5.39	5.96
Eu	1.03	1.02	0.91	0.79	1.08	1.69	1.081	1.13
Gd	4.58	4.57	4.23	3.67	5.10	6.74	5.13	5.39
Tb	0.80	0.82	0.80	0.70	0.84	0.99	0.88	0.87
Dy	5.08	5.23	5.42	5.02	5.13	5.16	5.67	5.21
Ho	1.08	1.15	1.20	1.14	1.04	0.99	1.16	1.06
Er	2.81	3.06	3.26	3.13	2.58	2.34	3.054	2.66
Tm	0.43	0.47	0.51	0.51	0.33	0.28	0.42	0.35
Yb	2.76	2.94	3.28	3.44	2.19	1.75	2.70	2.25
Lu	0.42	0.45	0.49	0.54	0.31	0.25	0.39	0.32
Hf	5.18	7.52	10.23	8.27	5.63	6.13	6.99	5.98
Ta	1.023	0.83	1.02	1.08	2.31	0.74	2.072	1.62
Pb	16.17	15.44	21.50	14.58	6.27	11.81	8.23	6.74
Th	31.60	31.24	39.16	36.47	13.00	20.05	14.30	12.09
U	0.99	1.68	1.29	1.52	1.16	2.087	1.37	1.26
(La/Sm) <sup>N</sup>	3.25	3.38	3.52	3.21	3.53	4.85	3.37	3.56
(Gd/Yb) <sup>N</sup>	1.37	1.28	1.06	0.88	1.93	3.19	1.57	1.98
(La/Yb) <sup>N</sup>	7.3	7.08	5.94	4.11	10.18	26.31	7.48	10.49
Eu/Eu*	0.62	0.60	0.59	0.62	0.61	0.68	0.62	0.6
Zr/Sc	19.86	24.25	30.66	27.63	10.1	21.93	15.4	16.58
Th/Sc	4.15	3.33	3.99	3.88	0.62	1.78	0.83	0.87
Th/Co	2.95	1.37	1.81	1.63	0.74	1.46	0.61	0.66
La/Th	0.88	0.93	0.69	0.54	2.39	3.19	1.96	2.72
La/Sc	3.69	3.1	2.77	2.1	1.48	5.71	1.62	2.39
Cr/Th	1.51	1.50	1.21	1.33	15.96	7.34	11.52	10.95

$$\text{Eu/Eu}^* = (\text{Eu})_N / \sqrt{(\text{Sm}_N * \text{Gd}_N)}$$

All analysed calc-silicates contain minor elements K, Na, Ti, and P in oxide-amounts less than 3 wt. %.K, Ti and P are present in similar amounts as compared to the composition of PAUCC whereas Na is generally depleted relative to PAUCC.Loss on ignition (LOI) measurements range from 0.44-2.05 %.

### **6.3 Trace and rare-earth elements compositions**

Analysed calc-silicate rock samples show concentrations of Zn(59-241 ppm), Ga(15.4-50.2 ppm) and large-ion-lithophile elements (LILEs) viz. Rb(73.7-1547.7 ppm), Ba(87-2076 ppm) and Th (12.1-66.5 ppm) and high field strength elements (HFSEs) viz. Zr (150.9-467.8 ppm), Nb (13.4-29.8 ppm) Hf (5.1-15.0 ppm) which are higher compared to the PAUCC whereas the same are generally depleted in V(35 -101 ppm), Cr (41-208 ppm),Ni (24.5-113 ppm),Cu (10.2-77 ppm) along with other LILEs i.e. Sr (90.1-206.3 ppm) and U(0.9-3.0 ppm). Similarly, analyzed calc-silicates have concentrations of Co (10.6-24.4 ppm), another LILEs such as Cs (0.50-11.03 ppm), Pb (6.2-29.1 ppm) and another HFSE viz.Ta (0.7-2.3 ppm) similar to PAUCC.

Rare-earth elements (REEs) are extremely useful in the studies of provenance of sedimentary rocks. (Lahtinen et al., 2002; Nesbitt 1979; Paikaray et al., 2008; Taylor et al., 1986) because of their insolubility and tendency to remain unfractionated in the supra-crustal environments (Nance and Taylor 1977).The analysed rock samples show LREE-enriched but HREE-depleted subparallel chondrite-normalized REE patterns with moderately negative Eu anomalies (Eu/Eu\*) ranging from 0.5 to 0.7 (Fig 6.2).

Similarly, according to Taylor and McLennan (1985), negative Eu-anomaly is suggestive of a typical continental crust composition and is also a characteristic of post-archean sedimentary rocks, thus supplementing the fact that sedimentary protolith for the these calc-silicates must be of post-archean age.

As the plagioclase is a host mineral for Eu, its weathering and Eu-depleted source rocks may affect the intensity of negative Eu anomaly. These rocks reveal fractionated REE patterns ( $La_N/Yb_N = 4.1$  to 26.3) with higher total REE abundances (up to 371 ppm).

REE patterns (including Eu anomalies) are influenced not only by provenance/source area and sedimentary environment but by the climatic conditions also, prevailing at the time of deposition of rocks (Yanjing and Yongchao, 1997).

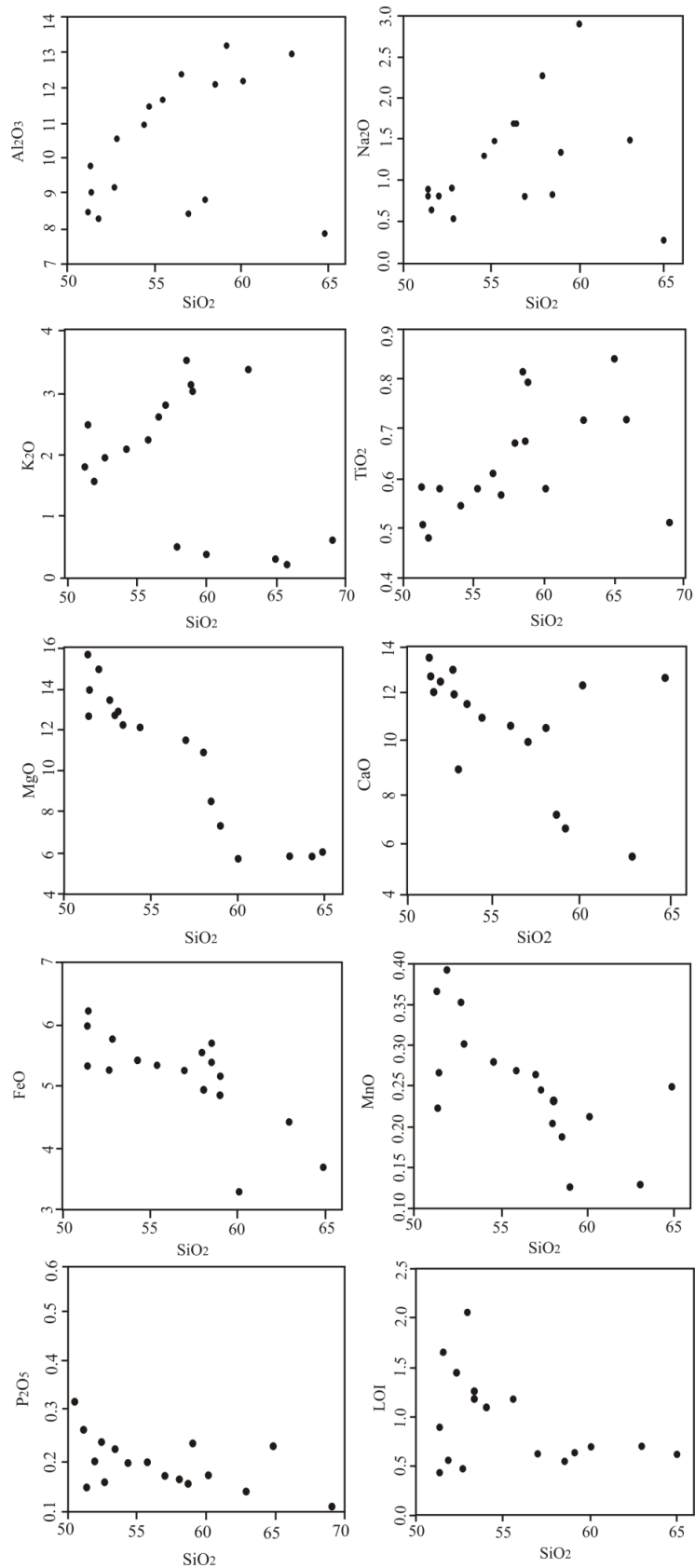


Figure 6.1: Whole-rock concentrations of major-element vs. silica in weight percent oxides for calc-silicates samples of Lunavada. Concentrations of all major elements excluding Al<sub>2</sub>O<sub>3</sub>, K<sub>2</sub>O, Na<sub>2</sub>O and TiO<sub>2</sub> exhibit near-linear inverse correlations with SiO<sub>2</sub>. \*All iron is reported as FeO.

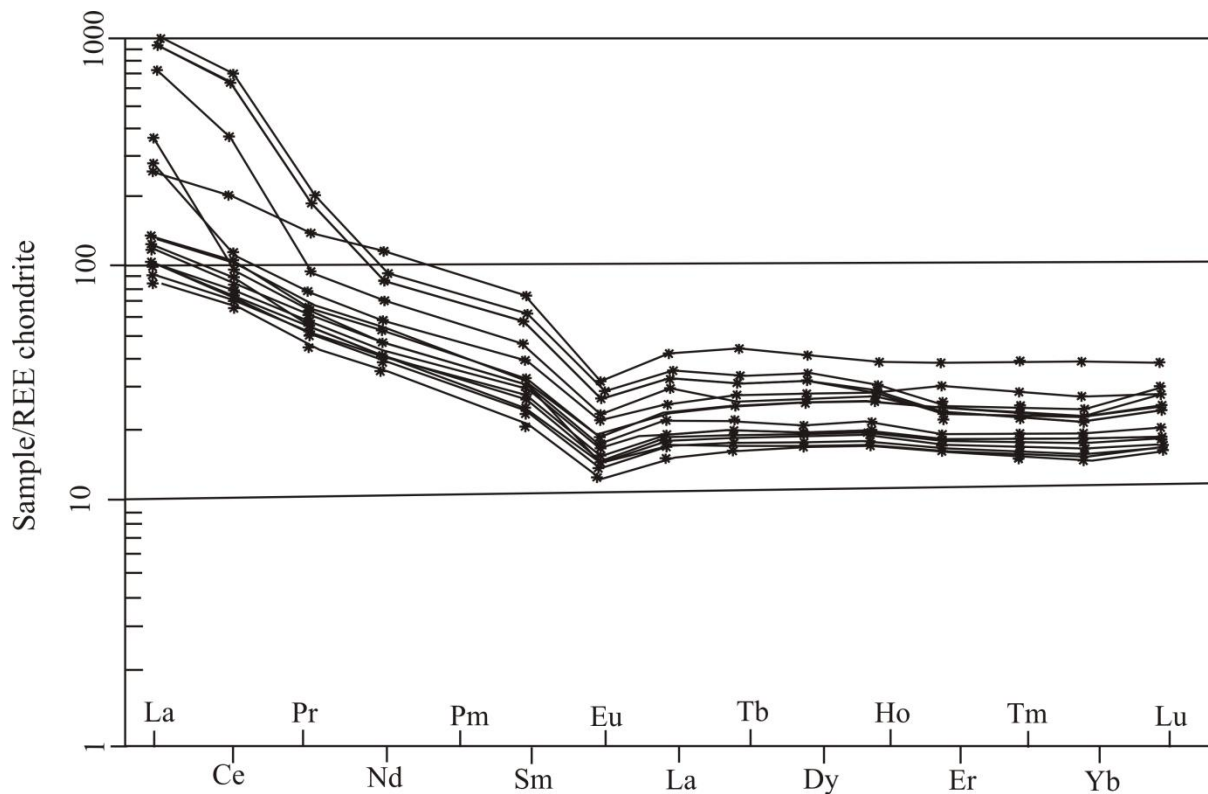


Figure 6.2: Chondrites normalized rare earth element (REE) patterns for calc-silicates of the study area (after Sun and McDonough, 1989).

Based on the studies of the early Precambrian sediments from the North China craton, these workers have convincingly argued that the high total REE and Eu depletion are the characteristics of the sediments deposited in oxidizing conditions (i.e.  $fO_2$  is high), similarly, reverse being true. Banded iron formations, red beds etc. found to be residing within the Proterozoic rocks from all over the world also supports this concept.

Interpretation of whole rock geochemistry data assisted in the determination of protolith, weathering history, provenance and tectonic setting of these rocks which is discussed in following sections.

#### 6.4 Protolith of calc-silicate rocks

Mobility of some elements such as Si, Na, K, Ca, Mg, Rb, and Sr of parent material of these calc-silicates might have affected remarkably due to certain metamorphic events and other alterations. Hence comparatively immobile elements such as the HREEs, HFSEs, Cr, Co, Th and Sc can be considered most reliable for protolith determination (Taylor and McLennan 1985; Bhatia and Crook 1986). They are insensitive to the igneous and

sedimentary fractionation processes (Garcia et al., 1991; McLennan et al., 1993; Garcia et al., 1994; Polat and Hoffman 2003) and generally transfer to the sediments quite unfractionated during sedimentary processes thus leaving the signatures of parent material or protolith within those sediments (Nance and Taylor 1977; Taylor and McLennan 1985; McDaniel et al., 1994).

Relative proportions of major oxides such as SiO<sub>2</sub>, CaO, Al<sub>2</sub>O<sub>3</sub>, FeO, and MgO reveal whether the calc-silicates possess a carbonate/silicate-rich clastic protoliths or metasomatic origins (Barton et al., 1991; Tracey and Frost 1991). Calc-silicate bulk-rock compositions normalized to CaO, Al<sub>2</sub>O<sub>3</sub>, and FeO + MgO are in agreement with the compositions of marls and calcareous sandstone (Pettijohn, 1984). On CaO, Al<sub>2</sub>O<sub>3</sub> and FeO + MgO ternary diagram, most of the calc-silicate samples fall within or very near to greywacke zone (Fig 6.3). Hence, the near-linear inverse correlation of CaO, MgO, FeO, MnO, P<sub>2</sub>O<sub>5</sub> and LOI with SiO<sub>2</sub> observed within sample areas may therefore be due to quartz dilution related to variable amounts of quartzo-feldspathic material and clay within protolith.

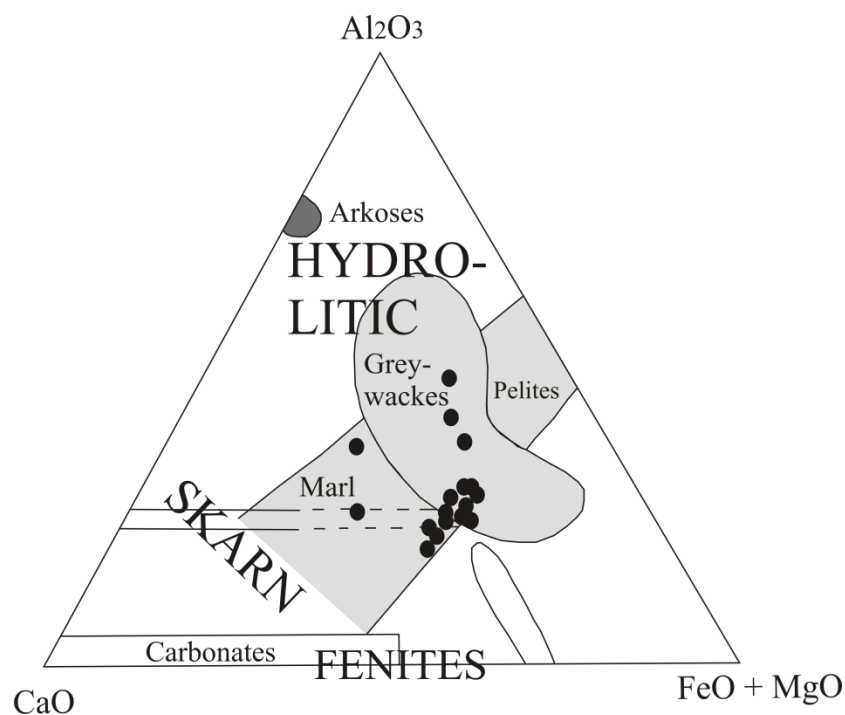


Figure 6.3: The bulk-rock compositions of calc-silicates are plotted on a CaO-Al<sub>2</sub>O<sub>3</sub>-FeO+MgO (wt. %) ternary diagram. General bulk compositions of unaltered arkoses, pelites, greywackes and marls are represented by shaded fields along with schematic regions for metasomatic types (after Barton et al., 1991).

$\text{Al}_2\text{O}_3$  is positively correlated with nearly all measured trace elements implies that these elements are primarily controlled by the potash-bearing minerals i.e. clay minerals and micas. Similarly, positive correlation of  $\text{Al}_2\text{O}_3$  with  $\text{Na}_2\text{O}$  and  $\text{K}_2\text{O}$  indicates that the potash-bearing minerals exert significant control over the Al distribution (Fig 6.4), thus further suggesting that the protolith must have been bound to clay (McLennan et al., 1990; Condie et al., 2001).

An enrichment of heavy mineral zircon in these calc-silicates is often due to its accumulation with quartz in the sand fraction during sedimentation and recycling (Taylor and McLennan, 1985; McLennan, 1989; McLennan et al., 1990). Similarly, enrichments of Ba in silica-rich samples indicate that Zr and Ba are positively correlated with  $\text{SiO}_2$ . Ba is also having positive correlation with  $\text{K}_2\text{O}$  may reflect a celsian component in detrital potassium-feldspars and deposited with quartz in the sandy portion of the protolith, as potassium-feldspar is more resistant to chemical weathering than plagioclase (Nesbitt and Young, 1989). In these rocks abundant microcline is present.

This fact supports the hypothesis of accumulation of potash feldspar in fluvial sands on account of source which must be mostly granitic (Nesbitt et al., 1996).

In the study area, the quartzite-metapelite sequence suggests the transition from sandstone to shale which denotes the sedimentary facies transitions from shallow-water shelf deposits to deep-water slope deposits. As the calc-silicate samples fall closer to sandstone zone on the Al-Zr-Ti diagram (Fig 6.5) of Garcia et al., (1994) which shows a sandstone-shale continuum, shallow-water shelf depositional environment is indicated for primary sediments.

Near linear variation of sample plots on this sandstone-shale continuum reflects the bimodal character of these rocks due to alternating cycles of sandstones and shale deposition, across strike within the study area which again supports the protolith having mixture and varying proportions of quartzo-felspathic material and clay.

Finally, it can be concluded that the protolith of calc-silicate rocks of the study area must be calcareous sandstone with small and varied amounts of clay within it

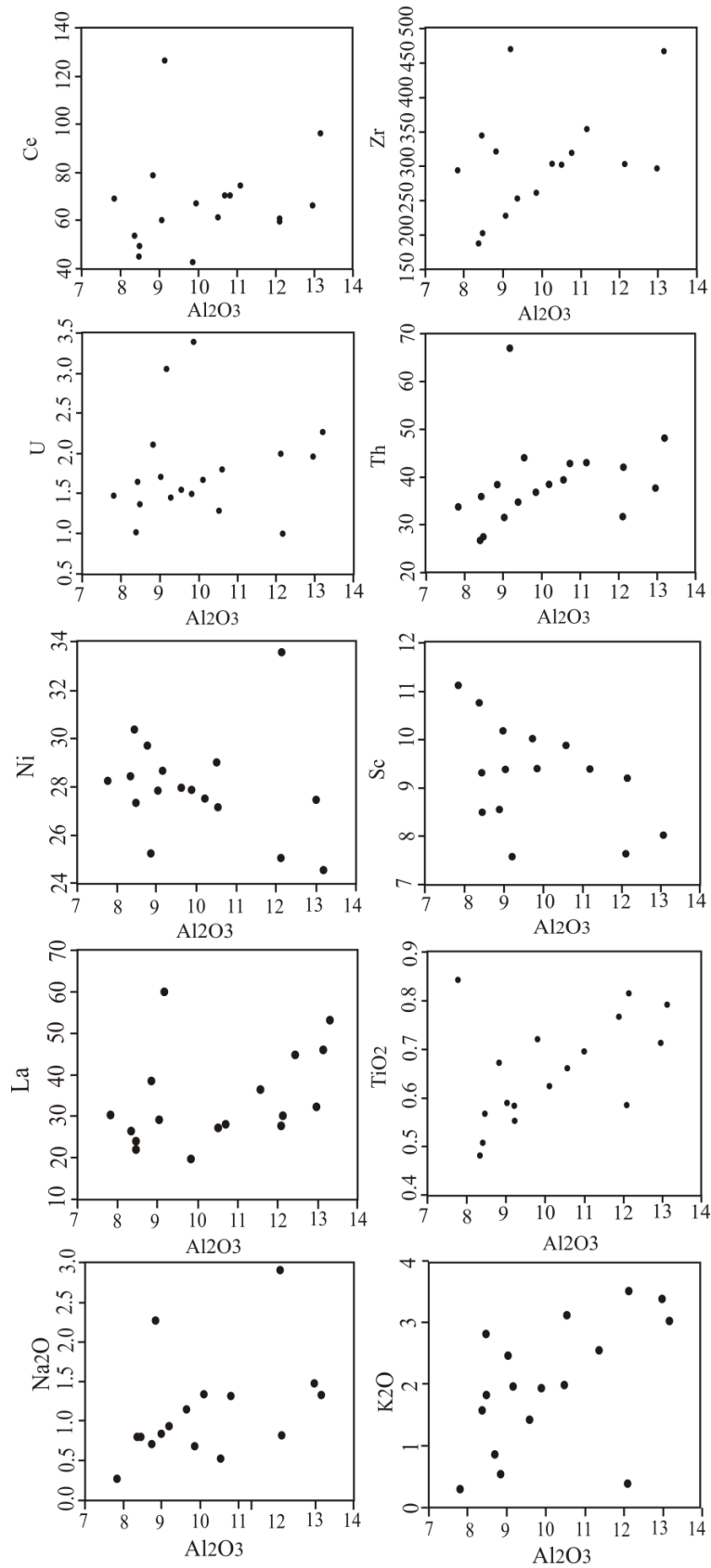


Figure 6.4: Whole-rock compositions of selected trace-elements along with  $Na_2O$  and  $K_2O$  exhibit a positive correlation with  $Al_2O_3$  in these calc-silicates (with the exception of Sc and Ni) suggesting these components were bound in clays.

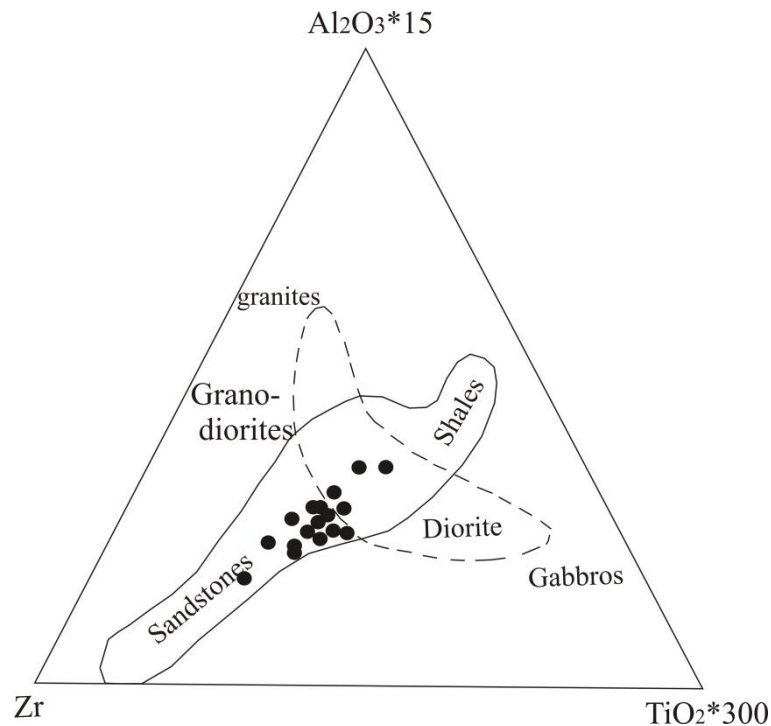


Figure 6.5: Whole-rock compositions of calc-silicates fall within the continuum between sandstone and shale (grey) on a ternary Al-Zr-Ti diagram (after Garcia et al.,1994). The field outlined by the dashed line represents the typical curved trend exhibited in whole-rock compositions of rocks derived from calc-alkaline plutonic suites.

### 6.5 Source area weathering

The mineralogy and physical properties of parent rocks as well as climatic conditions greatly affect the weathering of the source rocks. According to Sawyer (1986) and Nesbitt et al.,(1996), weathering in source area ultimately affects the composition of clastic sedimentary rocks or the protolith of any metamorphic rock.

Nesbitt and Young (1982) proposed the Chemical Index of Alteration (CIA) as a measure of the degree of chemical weathering/alteration of the source rocks. They have put forward the calculation where CIA is equal to  $[Al_2O_3 / (Al_2O_3 + CaO^* + Na_2O + K_2O)] * 100$ . The values of oxides are in molecular proportions and  $CaO^*$  represents  $CaO$  in silicate minerals only. The CIA values for calc-silicate rocks were calculated and plotted in the conventional  $Al_2O_3 - (CaO + Na_2O) - K_2O$  (A – CN – K) ternary diagram (Fig 6.6). It has been observed that the calculated CIA values for calc-silicate rocks are low to moderate i.e. 50 to 86 with average = 68 which indicates low to moderate weathering. Most of the samples plot in the

upper part of the diagram having inclination towards the illitic composition, thus indicating moderate degree of alteration.

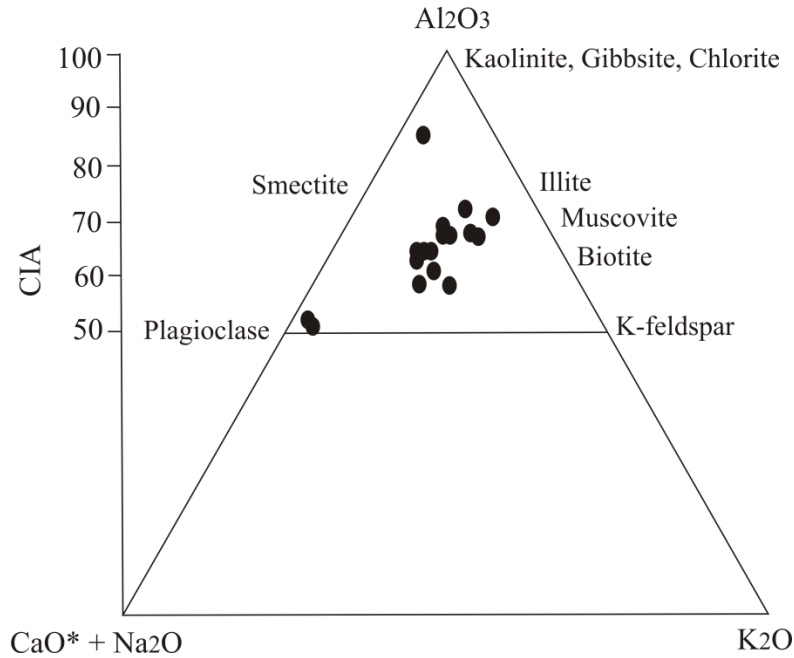


Figure 6.6: A-CN-K diagram (after Nesbitt and Young, 1982) using molar proportions of Al<sub>2</sub>O<sub>3</sub>, CaO, Na<sub>2</sub>O and K<sub>2</sub>O. As per the CIA scale, sample plots of calc-silicates indicate low to moderate and weathering of source rocks.

Low CIA values are the results of almost an absence of chemical alteration which may reflect cold and/or arid conditions or alternatively rapid physical weathering, probably in a subtropical condition (Singh and Khan, 2017). Thus cold and arid climatic conditions must have had a control over the weathering of source rocks for the calc-silicates under study. Major elements such as Ca, Na and K are highly mobile and are likely to be affected by weathering processes (Nesbitt et al., 1980; Nesbitt and Young, 1982), but Al<sub>2</sub>O<sub>3</sub> remains as a residual product as it is immobile relatively. With increase in weathering intensity, the rock becomes enriched in Al<sub>2</sub>O<sub>3</sub> relative to these mobile elements, thereby increasing its CIA.

### 6.6 Provenance

The immobile elements like Zr, Ti, Y, Nb, Cr, Sc, La, Th, Ce and Nd are often used to infer the paleo-tectonic environments of metamorphic rocks (Nutman et al., 2010; Giere et al., 2011), apart from their role in protolith determination. Th/Sc ratio is directly proportional

to Zr/Sc ratio during igneous differentiation, but as zircon enrichment in sediments affects this relation, Th/Sc vs. Zr/Sc diagram (McLennan et al., 1993) also serves as a good indicator to assess the sediment recycling (Ahmad et al., 2016). The Th/Sc– Zr/Sc plot (Fig.6.7) is used to discriminate evolved and juvenile sediment sources and the extent of sorting and recycling experienced by sediments (Taylor and McLennan 1985; McLennan et al., 1990), thus distinguishing the effects of source composition and sedimentary process on the basis of assumption that quartz dilution would result in preferential enrichment in Zr and to some extent, in Th (McLennan and Taylor, 1991).

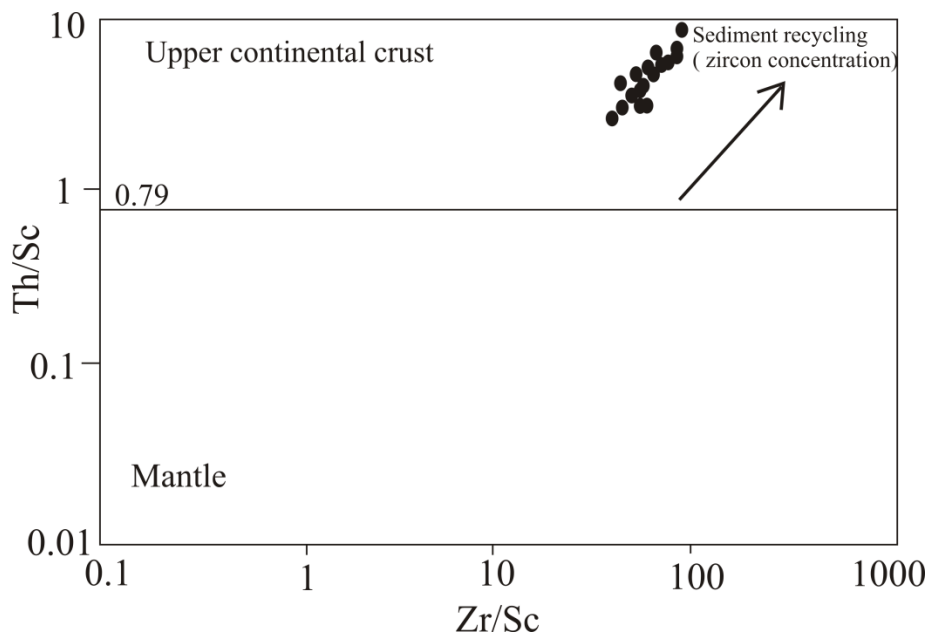


Figure 6.7: Th/Sc vs Zr/Sc ratio diagram showing the composition of the sources for the primary sediments of calc-silicate rocks and the extent of recycling or concentration of Zr in sediments, associated with the abundance of heavy minerals, particularly zircon (after McLennan et al., 1990).

This is based on the general trend of higher Th/Sc ( $\geq 1$ ) and Zr/Sc ( $\geq 10$ ) values in sediments derived from evolved continental sediment sources relative to sediments supplied by juvenile, mafic sources (Roser et al., 1996). Detritus from felsic rocks of the UCC have an average ratio equal to or greater than 0.79, while values less than 0.6 suggest mafic and ultramafic components (McLennan et al., 1990).

The calc-silicates under study exhibit Th/Sc ratio of greater than 0.79 thus suggesting a provenance from a felsic source. Similarly, detritus derived from a felsic source tend to be enriched in incompatible elements like Th, Zr and La, whereas those derived from

a mafic source are enriched in compatible elements like Sc, Cr and Co (Ahmad et al.,2016). Here it has been observed that these calc-silicates show enrichment in the incompatible elements viz. Th, Zr and La while they are depleted in Sc, Cr and Co, thus emphasizing the felsic nature of provenance.

Apart from Th/Sc, other elemental ratios between immobile elements such as La/Sc, Th/Co, and Cr/Th are the robust indicators of provenance (Wronkiewicz and Condie, 1990; Cullers, 1994). Th/Sc (2.4-8.8), La/Sc (2.1-8), Th/Co (1.1-3.6) and Cr/Th (0.8-1.7) ratios also support the sediment derivation from mostly homogeneous sources with major contribution from the felsic component. Calc-silicate samples fall in an array indicative of felsic composition of the source rocks in Th/Co vs. La/Sc bivariate plot i.e.(Fig.6.8) (Cullers, 2002).

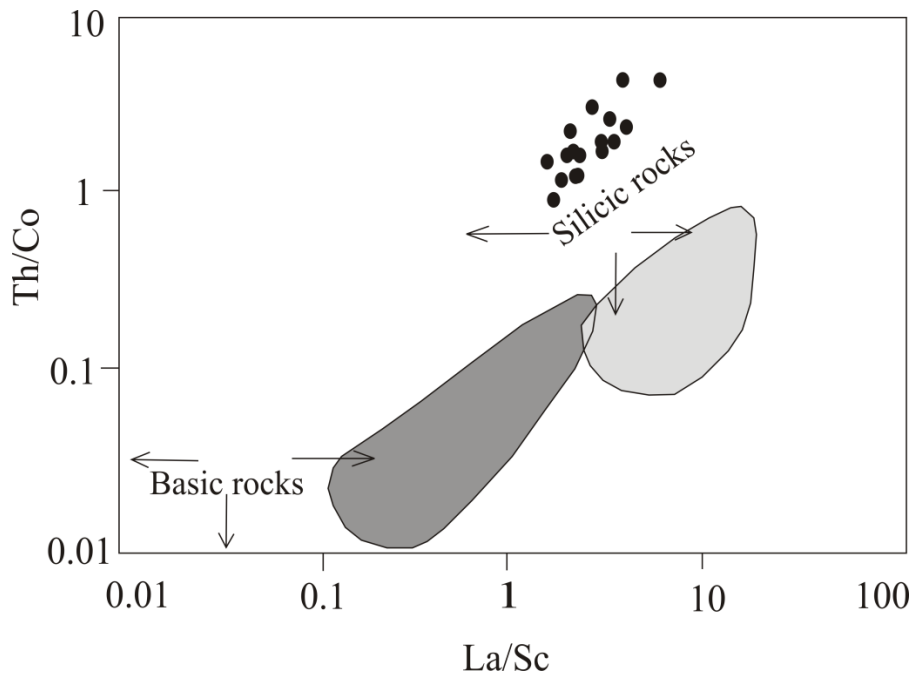


Figure 6.8: Th/Co vs. La/Sc diagram (after Cullers, 2002) where sample data plotted show affinity towards the source rocks of homogeneous composition of felsic nature.

Trace element studies revealed that the source of these calc-silicates was similar in composition to the average post-archean upper continental crust, mostly granitic thus supporting an idea that a significant amount of differentiated felsic igneous rocks probably present in the source area at the beginning of sedimentation.

## 6.7 Tectonic setting

The geochemistry of sedimentary rocks or of protolith is highly influenced by the tectonic settings in which they are deposited (Bhatia and Crook, 1986; Roser and Korsch, 1986; McLennan et al., 1990).

The immobile trace elements (as mentioned earlier) are also used to determine the paleo-tectonic setting of clastic sediments (Bhatia and Crook, 1986; McLennan et al., 1990). Here, Sc- Th- Zr/10 plot of Bhatia and Crook (1986) has been used because it can distinguish the sediments from passive margin to active continental margin settings. It can be seen that all the data fall within the field of active continental margin on this diagram (Fig. 6.9). Deposited sediments at the active continental margin are poorly sorted, less recycled and show less maturity than those deposited at the passive continental margin (Roser et al., 1996).

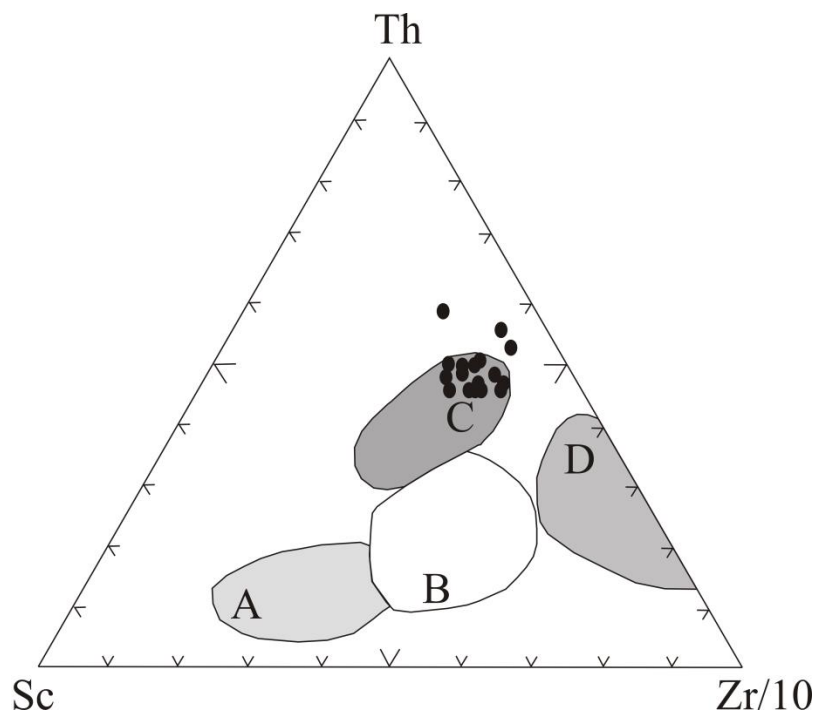


Figure 6.9: Sc-Th-Zr/10 diagram of Bhatia and Crook (1986), A: oceanic island arc; B: continental island arc; C: active continental margin D: passive/rifted margins; calc-silicate samples fall in the 'C' region of this diagram indicating deposition of primary sediments in active continental margin setting.

----- END -----